

COVER PAGE

Document downloaded by @DAEL

Fri Nov 27 15:44:33 2026
For personal use

When automatic English translation is provided, only the original document is authentic.
The EAA cannot be held responsible of any translation error

Bibliographical reference

Efficiency of Energy Radiation from an Unflanged Cylindrical Duct in Case of Multimode Excitation, Anna Snakowska and Jerzy Jurkiewicz, Acta Acustica **vol. 96** (Number 3), 2010, pp. 416-424

DOI
https://doi.org/10.3813/AAA.918294

Acta Acustica united with Acustica
Vol. 96 (2010) 416 – 424

DOI 10.3813/AAA.918294

Efficiency of Energy Radiation from an Unflanged Cylindrical Duct in Case of Multimode Excitation

Anna Snakowska[1)], Jerzy Jurkiewicz[2)]

[1)] Faculty of Mechanical Engineering and Robotics, AGH, Al. Mickiewicza 30, 30-059 Cracow, Poland. anna.snakowska@agh.edu.pl

[2)] Faculty of Electrical Engineering Automatics IT and Electronics, AGH, Al. Mickiewicza 30, 30-059 Cracow, Poland. jurkiewi@agh.edu.pl

Summary

The aim of this paper consists in presentation of spatial distribution of energy radiated from the outlet of a cylindrical duct in case of multimodal excitation. As the mathematical model, the semi-infinite unflanged hard duct was applied, so the results account for the diffraction phenomena occurring at the duct opening. They are based on solution of the wave equation with Neumann boundary conditions obtained by means of the Wiener–Hopf method. The multimode excitation was considered assuming the incident wave composed of all propagating modes representing solutions of the wave equation at a given diffraction parameter (Helmholtz number) and equal energy per mode (EEpM) allowing to derive mode amplitudes. The paper presents mathematical formulae and numerical results for the power radiated outside, the power reflection coefficients and the power-gain function for different values of the diffraction parameter ka. The presented results can be applied for modeling of passive and/or active noise reducing systems

PACS no. 43.20.Mv, 43.20.Rz

1. Introduction

In acoustics, the most frequently discussed types of ducts are those with absolutely rigid (hard) or sound absorbing walls. Rigid ducts are of particular interest as components of heating and ventilation systems, aircraft jet engines etc. where additionally flow of the medium takes place. As such devices are often sources of harmful environmental noise, there is a strong pressure on manufactures to reduce the emitted noise. In recent decades it resulted in growing interest in duct acoustics, what in turn led to new theoretical solutions used in modeling of the acoustic field inside and outside the duct with increasing accuracy, and numerous applications of new techniques. The flanged duct model [1, 2], applied commonly for its relative simplicity, assumes radiation only into the front hemisphere and is not accurate enough, especially for angles to the duct axis exceeding 70°. The description of sound radiation from a duct end can be improved by accounting for diffraction phenomena at the outlet and the multimode excitation, which in fact takes place with the appearance of the first circumferential mode ($ka > 1.84$, k — wavenumber, a — duct radius). Both of these assumptions are particularly important e.g. when modeling the sound field of a jet engine, where the frequency considered is high and the duct radius is large. The results presented in this paper are based on exact solution of the wave equation with Neumann boundary conditions imposed on the semi-infinite duct obtained by means of the Wiener-Hopf method [3, 4] and factorization technique.

In parallel, some other techniques leading to accounting for the diffraction phenomena were developed. Chapman in his papers [5] and [6], based on the geometrical theory of diffraction (GTD) developed by Keller [7, 8], has built up a complete three-dimensional ray structure of the duct modes inside the duct and of the sound field radiated from its end. The rays, constituting linear helices inside the duct, produce at its end face the "Keller cones" of diffracted rays which, in turn, determine the structure of the radiated field. Chapman's approach has been successfully applied by many authors. Hocter compared the results of the exact solution obtained by means of the Wiener-Hopf method with the approximate results calculated according to Chapman's findings and the so-called Weinstein's U function [4], derived by simplifying the kernel factors appearing in the Wiener-Hopf technique. He analyzed the reflected field inside the duct [9] and also the power distribution in the far field [10, 11], which led him to the conclusion that these approximations were valid in most regions of the far field, providing the frequency was high. Peak and Keith [12, 13] considered high wavenumber acoustic radiation and appli-

Received 9 June 2009,
accepted 12 February 2010.

© S. Hirzel Verlag · EAA

cations of the high frequency asymptotics to the problem of sound produced by large modern aeroengines.

In duct-like devices such as jet engines, heating and ventilation systems, large chimneys etc. the flow of the medium takes place. If the flow is assumed to be of uniform velocity over the duct cross section [14, 15], with the Mach number $M < 1$, the phenomena induced by the flow can be accounted for by applying the Prandtl-Glauert transformation [15, 16] to the formulae derived herein. Thus, the results presented in this paper can also be applied to ducts with uniform flow velocity profile.

Multimodal excitation means that all propagating modes, representing admissible solutions of the wave equation at a given diffraction parameter ka (Helmholtz number), are present in the incident wave. This type of excitation is rather rarely discussed in papers on duct acoustics except for such papers as [17, 18, 19]. In one of them, Joseph and Morfey [17] noticed that most of the literature concerned with the radiation from ducts was restricted to individual modes.

For the sake of the quantitative field analysis the assumption of equal energy per mode (EEpM), making possible to determine amplitudes of consecutive modes, is adopted in the present paper. The power reflection r_{mll} and transformation (coupling) r_{mln} coefficients, together with the directivity d_{mln} functions calculated herein allow to evaluate the power remaining inside the duct and the power radiated outside, as well as the directivity characteristics of the pressure, of the intensity and of the power-gain function. The power-gain function $G(\theta, \varphi)$, determining directions corresponding to the strongest radiation, was first calculated by Levine and Schwinger in their pioneering paper on the semi-infinite cylindrical duct [20], in which they also derived the amplitude reflection coefficient of the plane wave R_{000}, omitting however the coupling coefficients between the plane wave and the higher radial modes. Later, the power-gain function was analysed by Weinstein [4], who pointed out its usefulness in checking accuracy of the results obtained - when integrated over the total solid angle the result should be 4π. The successive authors discussed the pressure/intensity directivity characteristics more often.

The results of this paper presenting spatial distribution of energy radiated from the duct outlet can be applied in calculating the aircraft engine sound field and modeling of both active [14] and passive [16] noise reducing systems.

2. Basic mathematical formulae

2.1. Wave equation and the Prandtl-Glauert transformation

The wave equation for the velocity potential in a duct with flow of the medium takes the form [21]

$$\left(\triangle - \frac{1}{c^2} \frac{D^2}{Dt^2} \right) \Phi(\mathbf{r}, t) = 0, \tag{1}$$

where $D/Dt = \partial/\partial t + \mathbf{u} \cdot \nabla$ is the so-called substantial derivative with respect to the flow velocity $\mathbf{u}$.

Assuming harmonic excitation with the angular frequency ω, flow of the medium in the z direction and the flow Mach number $M = u/c$, where c is the sound velocity and $k = \omega/c$ is the free space wavenumber, one obtains in the cylindrical coordinates (ϱ, φ, z) [21]

$$\frac{1}{\varrho}\frac{\partial}{\partial \varrho}\left(\varrho \frac{\partial \Phi}{\partial \varrho}\right) + \frac{1}{\varrho^2}\frac{\partial^2 \Phi}{\partial \varphi^2} + \frac{\partial^2 \Phi}{\partial z^2} - \left(-\mathrm{i}k + M\frac{\partial}{\partial z}\right)^2 \Phi = 0. \tag{2}$$

If the flow is uniform, the above equation can be reduced to the wave equation without flow for the velocity potential $\triangle \Phi^{fl} - c^{-2}\partial_{tt}\Phi^{fl} = 0$ by applying the Prandtl-Glauert transformation [16, 4]

$$\tilde{k} = \frac{k}{\sqrt{1-M^2}}, \quad \tilde{\gamma}_{mn} = \sqrt{\tilde{k}^2 - \frac{\mu_{mn}^2}{a^2}}, \tag{3}$$

$$\tilde{z} = \frac{z}{\sqrt{1-M^2}}, \quad \tilde{x} = x, \quad \tilde{y} = y. \tag{4}$$

Thus, in an infinite duct with uniform flow the velocity potential of a single (m, l) mode of amplitude A_{ml} is given by

$$\Phi_{ml}^{fl}(\varrho, \varphi, z, t) = A_{ml} \mathrm{e}^{\mathrm{i}(m\varphi - M\tilde{k}\tilde{z})} \cdot \left[J_m\left(\mu_{ml}\frac{\varrho}{a}\right) \mathrm{e}^{\mathrm{i}\tilde{\gamma}_{ml}\tilde{z}} \right] \mathrm{e}^{-\mathrm{i}\omega t}, \tag{5}$$

where J_m denotes the Bessel function of m-th order, $\tilde{\gamma}_{ml}$ — the axial wavenumber, μ_{ml}/a — the radial wavenumber, μ_{ml} — l-th root of the derivative $J'_m(x)$.

The formula for the velocity potential in an infinite duct with uniform flow differs from the corresponding formula in the absence of flow by the phase factor $\mathrm{e}^{-\mathrm{i}M\tilde{k}\tilde{z}}$ and substitution of the $\mathrm{e}^{\mathrm{i}\tilde{\gamma}_{ml}\tilde{z}}$ factor instead of $\mathrm{e}^{\mathrm{i}\gamma_{ml}z}$. One can expect that the acoustic potential in a semi infinite duct as well as the reflection/transformation coefficients, the far field directivity function and other physical quantities can be easily transformed to describe the sound field of the duct with flow.

2.2. Velocity potential. Amplitude reflection and transformation coefficients and the far field directivity functions

Elementary features of wave phenomena occurring in ducts can be briefly described as follows: for a duct excited with given frequency ω there is a limited number of propagating modes, depending on the duct radius a, thus the most adequate quantity for analyzing the in-duct phenomena is the diffraction parameter $ka = \omega a/c$, called also the reduced frequency or the Helmholtz number. The limit in the frequency domain between modes that can propagate freely and those exponentially attenuated is determined by the so called cut-off frequency.

The mode corresponding to the smallest eigenvalue is called the fundamental (principal) mode. For a rigid circular duct that is the plane wave with the cut-off frequency equal to zero.

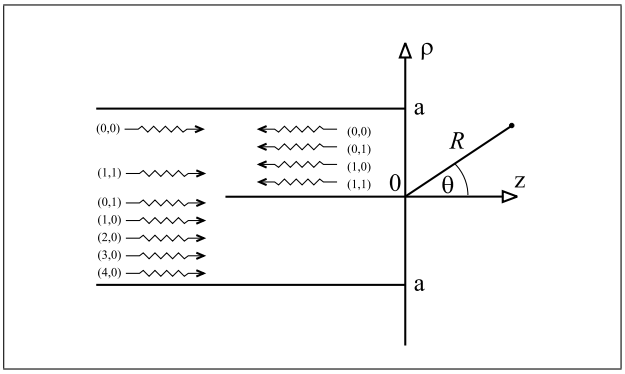

Figure 1. Geometry of a cylindrical duct in (ϱ, φ, z) coordinates.

In general, when harmonic excitation is considered with a given frequency ω, the incident wave, i.e. the wave heading the duct outlet, is a superposition of a number of cut-on (propagating) modes, the phenomenon being called the multimodal excitation. The acoustic potential of the incident wave is a sum of single mode potentials

$$\Phi^{inc}(\varrho, \varphi, z, t) = \sum_{m,l} \Phi^{inc}_{ml}(\varrho, \varphi, z, t). \tag{6}$$

The total resultant field can be expressed as a sum of the incident and diffracted field

$$\begin{aligned}\Phi(\varrho, \varphi, z, t) &= \Phi^{inc}(\varrho, \varphi, z, t) \\ &\quad + \Phi^{dif}(\varrho, \varphi, z, t).\end{aligned} \tag{7}$$

The time dependent factor $\exp(-\mathrm{i}\omega t)$ will be omitted for brevity in the following.

At the outlet, each of the incident modes (m, l) transforms, due to diffraction, into all cut-on modes of the same circumferential order, i.e. $(m, l) \to (m, n)$, thus the potential related to the single (m, l) incident mode of amplitude A_{ml} takes the form [3]

$$\begin{aligned}\Phi_{ml}(\varrho, \varphi, z) = A_{ml}\mathrm{e}^{\mathrm{i}m\varphi} \Bigg[&\frac{J_m\left(\mu_{ml}\dfrac{\varrho}{a}\right)}{J_m(\mu_{ml})}\, \mathrm{e}^{\mathrm{i}\gamma_{ml}z} \\ &+ \sum_{n=1/0}^{N_m} R_{mln} \frac{J_m\left(\mu_{mn}\dfrac{\varrho}{a}\right)}{J_m(\mu_{mn})}\, \mathrm{e}^{-\mathrm{i}\gamma_{mn}z} \Bigg],\end{aligned} \tag{8}$$

where the term under the sum sign corresponds to diffraction effects, summation starts from $n = 0$ only for $m = 0$ (the term with indices $(0, 0)$ represents the plane wave), N_m denotes the number of "higher modes" of circumferential order m at a given ka, R_{mln} — the wave amplitude reflection/transformation coefficient, explicit formulae for which can be found in [3, 4, 9]. In the present paper a number of plots for asymmetric modes is included and compared with corresponding power reflection/transformation coefficients.

The velocity potential inside the duct, in the presence of flow characterized by Mach number M, is given by

$$\begin{aligned}\Phi^{fl}_{ml}(\varrho, \varphi, z) = A_{ml}\mathrm{e}^{\mathrm{i}(m\varphi - M\tilde{k}\tilde{z})} \Bigg[&J_m\left(\mu_{ml}\frac{\varrho}{a}\right)\mathrm{e}^{\mathrm{i}\tilde{\gamma}_{ml}\tilde{z}} \\ &+ \sum_{n=0/1}^{\tilde{N}_m} \tilde{R}_{mln} J_m(\mu_{mn}\frac{\varrho}{a})\mathrm{e}^{-\mathrm{i}\tilde{\gamma}_{mn}\tilde{z}} \Bigg],\end{aligned} \tag{9}$$

where $\tilde{R}_{mln}$ denotes the transformation/coupling $(l \neq n)$ or reflection $(n = l)$ coefficient calculated according to the Prandtl-Glauert transformation formulae (3), (4).

The far field outside the duct, at a distance R, which mathematically, is a product of the directivity function d_{ml} and the point source velocity potential

$$\Phi_{ml}(R, \theta, \varphi) = d_{ml}(\theta, \varphi)\frac{\mathrm{e}^{\mathrm{i}kR}}{R}, \tag{10}$$

becomes, in the duct with uniform flow,

$$\Phi^{fl}_{ml}(R, \theta, \varphi) = A_{ml}\tilde{d}_{ml}(\theta, \varphi)\frac{\mathrm{e}^{\mathrm{i}(\tilde{k}\tilde{r} - M\tilde{k}\tilde{z})}}{\tilde{r}}, \tag{11}$$

where, as before, the tilda sign indicates calculations with respect to the Prandtl-Glauert transformation formulae (3), (4) and $\tilde{r} = \sqrt{x^2 + y^2 + \tilde{z}^2}$. Explicit formulae of the directivity coefficients d_{ml} which are, by definition, the pressure directional characteristics of the outlet radiation, can be found in [4, 22, 23].

For circumferential modes $(m \neq 0)$ it is suitable to express the directivity functions as

$$d_{ml}(\theta, \varphi) = d_{ml}(\theta)\cos(m\varphi). \tag{12}$$

Derivation of the amplitude reflection/coupling coefficients and the far field directivity functions form a base for numerical computations and further sound field analysis, especially in the scope of the acoustic energy spatial distribution.

Comparing Figure 2 with Figure 3 it can be seen that for ka slightly exceeding the cut-on frequency, the transformation coefficients $R_{5,n,1}$ and $R_{5,1,n}$ differ significantly. Transformation of modes $(1 \to n)$ is strongest just above the cut-on frequency and decreases significantly with ka. On the contrary, the $(n \to 1)$ coupling coefficient increases from zero for the cut-on frequency to values approximately achieved by the $(1 \to n)$ coefficient. For $ka \gg \mu_{mn}$, the reflection coefficient exceeds any of the transformation coefficients, which in turn approach the same asymptotic value, thus making possible to apply the approximate formulae [11, 12, 13]. The amplitude reflection coefficients R_{mnn}, equal to one at the cut-on frequency quickly decrise with increasing frequency, however the lowest/principal mode of order m — mode $(m, 1, 1)$ is refleced better than any other. All of them reveal their modal nature, with minima and maxima occurring according to consecutive cut-on frequencies.

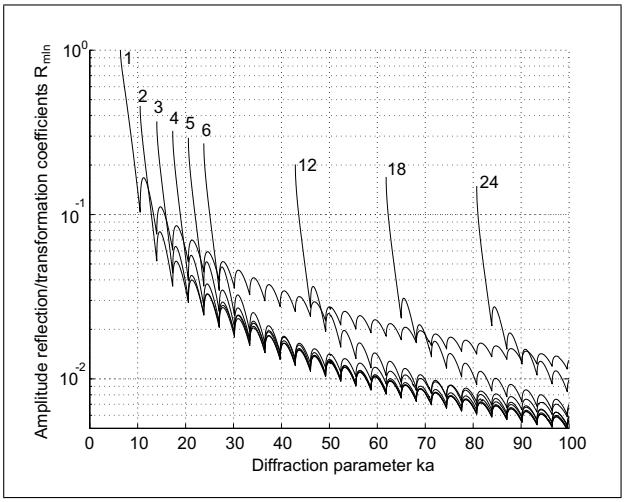

Figure 2. Amplitude reflection $R_{5,1,1}$ and transformation coefficients $R_{5,1,n}$ of the asymmetric mode $(5, 1)$ into higher order modes $(5, n)$. Numbers by the curves represent corresponding n values.

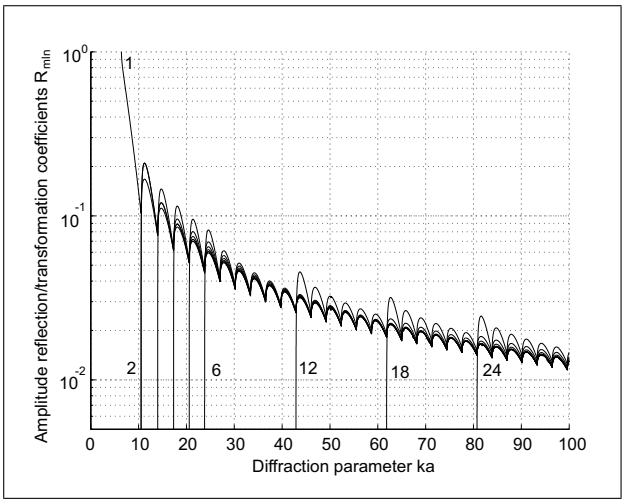

Figure 3. Amplitude reflection $R_{5,1,1}$ and transformation coefficients $R_{5,l,1}$ of the asymmetric mode $(5, l)$ into lower order modes $(5, 1)$. Numbers by the curves represent corresponding l values.

3. The acoustic energy spatial distribution

3.1. The power radiated outside

The power radiated outside the duct, representing the difference between the incident and the reflected power, $\mathcal{P}^{rad} = \mathcal{P}^{inc} - \mathcal{P}^{ref}$, can be easily expressed by the total power reflection coefficient r_{ml}, indicating what part of the incident power of the (m, l) mode returns to the duct in the form of all cut-on modes

$$\mathcal{P}^{rad}_{ml} = \mathcal{P}^{inc}_{ml}(1 - r^{tot}_{ml}). \tag{13}$$

Exact formula for the r^{tot}_{ml} coefficient will be derived below.

Using the definition of the acoustic power $\mathcal{P} = \int_S p v^*_n ds$, in the form of a surface integral of the acoustic pressure $p = \rho_0 \partial_t \Phi$, ($\rho_0$ — medium density) and the normal component of the particle velocity $\overline{v} = -\nabla\Phi$ [25], and applying the Bessel functions integration formula [24]

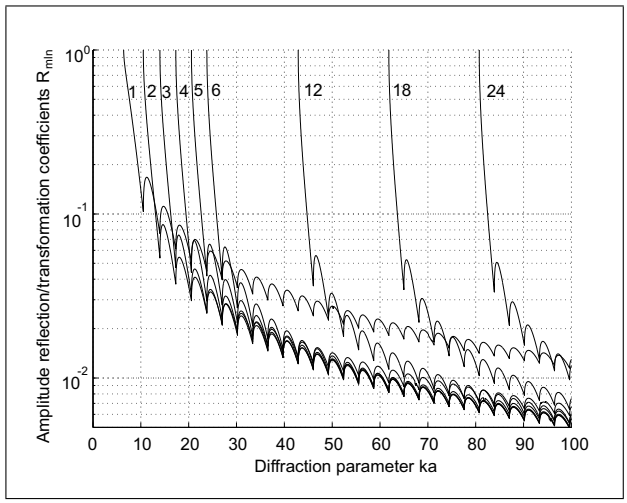

Figure 4. Amplitude reflection coefficients $R_{5,l,l}$ of the asymmetric modes $(5, l)$. Numbers by the curves represent corresponding l values.

$$\int_0^a J_m(\beta_{mn}\varrho) J_{m'}(\beta_{m'n'}\varrho)\varrho \, \mathrm{d}\varrho = \tag{14}$$
$$\begin{cases} \dfrac{a^2}{2}\left[J'^2_m(\beta_{mn}a)^2 + \left(1 - \dfrac{m^2}{\beta^2_{mn}a^2}\right)J^2_m(\beta_{mn}a)\right]\delta_{mm'}\delta_{nn'}, & \beta_{mn} > 0 \\ \dfrac{a^2}{2}, & \beta_{00} = \frac{\mu_{00}}{a} = 0, \end{cases}$$

where $\delta_{mm'}$ is the Kronecker delta function, the result is

$$\mathcal{P}^{rad}_{ml} = \frac{1}{4}\pi a^2 \rho_0 c k |A_{ml}|^2 \cdot \sum_{n=1/0}^{N_m} \gamma_{mn} \mathcal{W}(m, n)(\delta_{nl} - |R_{mln}|^2), \tag{15}$$

where

$$\mathcal{W}(m, n) = \begin{cases} 1 - \dfrac{m^2}{\mu^2_{mn}}, & m \neq 0, \\ 1, & m = 0. \end{cases} \tag{16}$$

From Figure 5 and Figure 6 it can be seen that above the mode cut-on frequency the amount of the power radiated outside increases rapidly and comes close to the maximum value with shallow minima at cut-on frequencies of the consecutive modes. The degree to which each mode contributes to the total radiated power depends on values of the reflection/transformation coefficients.

In case of multimodal excitation, as a result of the orthogonality of Bessel functions [24], the power of the incident wave is equal to the sum of mode powers. The amplitudes of modes are often derived assuming equipartition of the incident wave energy between the exited modes (EEpM — equal energy per mode). Mathematically, the

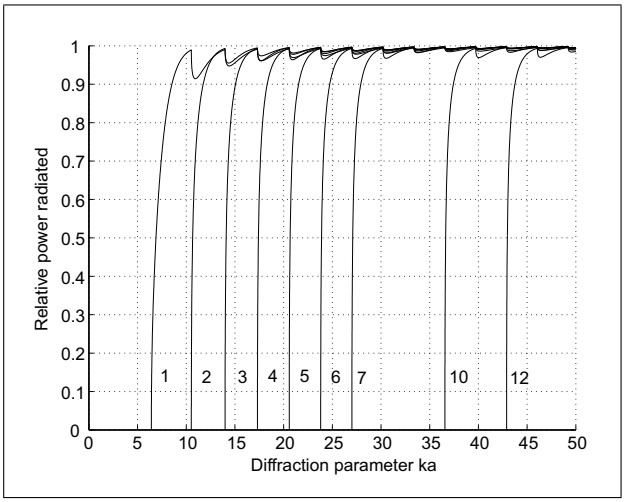

Figure 5. Relative acoustic power $\mathcal{P}^{rad}_{ml}/\mathcal{P}^{inc}_{ml} = 1 - r^{tot}_{ml}$ radiated outside by the incident asymmetric modes $(5, l)$. Numbers by the curves represent corresponding l values.

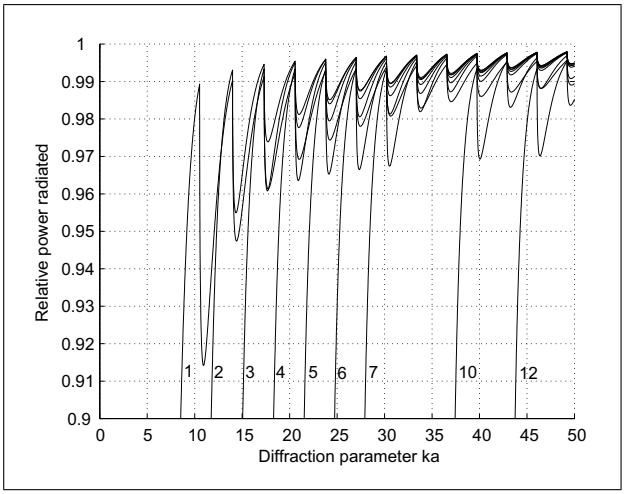

Figure 6. Same as Figure 5 but in different scale.

assumption is justified by the above mentioned properties of Bessel functions. It was also confirmed experimentally by Bolleter and Crocer [26] who found that the EEpM assumption is fulfilled with significant accuracy. Since then the EEpM model has been applied successfully in numerous papers on duct acoustics, e.g. [17, 18, 19], as a reasonable assumption one can adopt in constructing mathematical model of the phenomenon. The main result of this assumption is that it allows not only for qualitative, but also quantitative field analysis [27, 28], of great importance for testing theoretical models of duct-like devices, such as heating and ventilation systems, jet engines etc.

According to (14), for a given ka, the calculated amplitudes are equal to

$$|A_{mn}| = \sqrt{\frac{2\mathcal{P}^{inc}_{mn}}{\pi a^2 \rho_0 c k \gamma_{mn} \mathcal{W}(m,n)}}. \tag{17}$$

Analyzing the multimode excitation as a function of ka it is reasonable to assume the constant power of the incident

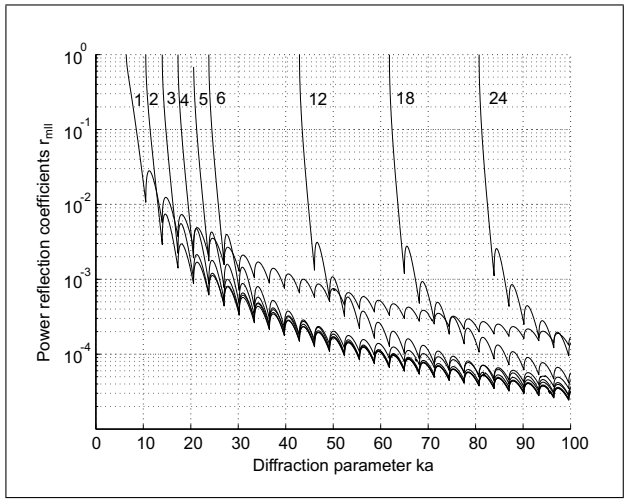

Figure 7. Power reflection $r_{5,l,l}$ coefficients of asymmetric modes. Numbers by the curves represent corresponding l values.

wave. Then, the modes amplitudes are given by the above formula, in which the $\mathcal{P}^{inc}_{mn}$ was replaced by $\mathcal{P}^{inc}/N_m(ka)$.

3.2. Power reflection/transformation coefficients

The power reflection/transformation coefficients r_{mln}, defined as the ratio of power of the excited mode (m, n) to the power of the incident mode (m, l) are symmetric, i.e. $r_{mln} = r_{mnl}$ and take the form

$$r_{mln} = \frac{\gamma_{mn}\mathcal{W}(m,n)}{\gamma_{ml}\mathcal{W}(m,l)}|R_{mln}|^2, \tag{18}$$

thus, the power radiated outside for single mode excitation can be expressed as

$$\mathcal{P}^{rad}_{ml} = \mathcal{P}^{inc}_{ml}(1 - \sum_{n=1}^{N_m} r_{mln}). \tag{19}$$

The last rule does not apply to multimodal excitation — as it will be shown in what follows, the radiated power $\mathcal{P}^{rad}_{m}$ is not simply a sum over l of the (19).

The r^{tot}_{ml} coefficient, called the total power reflection coefficient [4], indicates which part of the incident power of the (m, l) mode returns to the duct in the form of all cut-on modes

$$r^{tot}_{ml} = \sum_{n=0/1}^{N_m} r_{mln}, \tag{20}$$

and so

$$\mathcal{P}^{rad}_{ml} = \mathcal{P}^{inc}_{ml}\left(1 - r^{tot}_{ml}\right). \tag{21}$$

Analysis of the presented figures (Figure 7, Figure 8) and many others, not included in the paper, leads to the conclusion that the power reflection coefficients are close to unity when ka exceeds slightly the cut-on value, which means that nearly all energy returns to the duct and radiation outside is weak. With increasing ka, reflection coefficients quickly decrease to $10^{-2} \div 10^{-4}$, demonstrating at

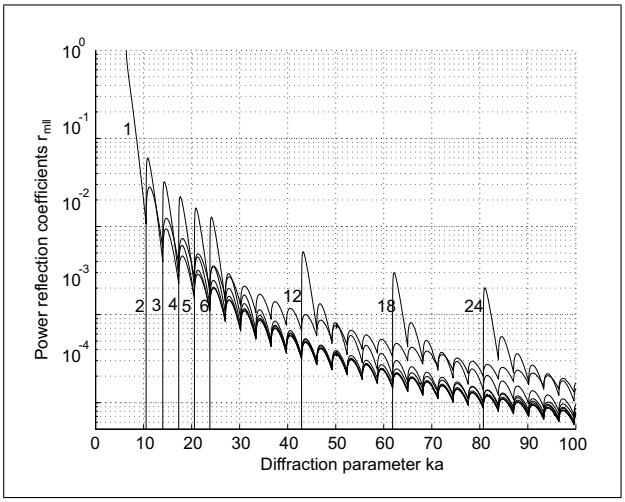

Figure 8. Power reflection $r_{5,l,l}$ and transformation $r_{5,1,n} = r_{5,n,1}$ coefficients of asymmetric modes. Numbers by the curves represent corresponding n values.

the same time their modal nature by achieving minima and maxima in accordance with appearance of the successive modes. That means that the modal reflection coefficients are in general negligible except for the region close to the cut-on frequency. Apart from this range of frequency the wave energy is efficiently radiated outside. On the contrary, values of the power transformation coefficient are small just above the cut-on frequency (when the reflection coefficients are relatively large), then increase rapidly and for a given m their maxima diminish with the radial mode index n.

3.3. The power-gain function

The power-gain function is one of directivity functions, such as the pressure or the intensity directivity functions. As it was mentioned in the Introduction, the function was discussed by Levine and Schwinger [20] and Weinstein's [4] in their fundamental papers on duct acoustics. It is defined as the power density (intensity) radiated into a unit solid angle in the given direction to the average power radiated into a unit solid angle. It differs from the intensity directivity function only by a constant, but it fulfils a relation useful for checking the accuracy of the results obtained - when integrated over the total solid angle it equals 4π. This allows to check the correctness of the derived mathematical formulae for the reflection coefficients R_{mln} and the directivity functions $d_{ml}(\theta, \varphi)$ as well as the accuracy of the numerical calculations. The power-gain function indicates how strong the radiation in a given direction is, compared to the radiation of an omnidirectional source of the same power output and so determines directions of strong and weak power radiation. Its derivation may be of great interest for the sound field analysis, especially in environments close to airports, areas with running combustion engines etc.

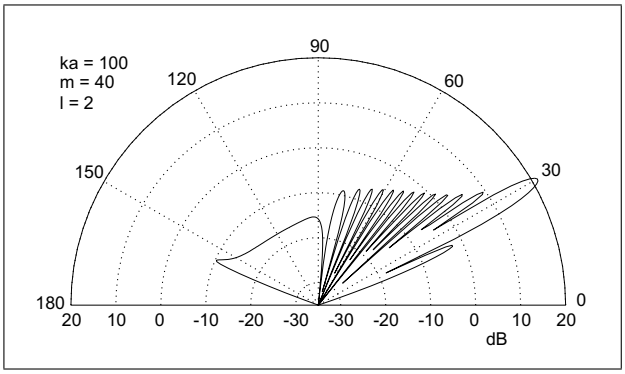

Figure 9. Power-gain function $G_{40,2}(\theta)$ for the diffraction parameter $ka = 100$ above the cut-on frequency of the (40, 15) mode.

In case of multimodal excitation the power radiated outside calculated at the duct outlet is

$$\mathcal{P}_m^{rad} = \frac{1}{4}\pi a^2 \rho_0 c k \sum_{l=1/0}^{N_m} \gamma_{ml} \mathcal{W}(m,l)\left(|A_{ml}|^2 - |B_{ml}|^2\right), \quad (22)$$

where B_{ml} represents the amplitude of the (m, l) mode returning to the duct as a result of mode coupling

$$B_{ml} = \sum_{n=1/0}^{N_m} A_{mn} R_{mnl}. \quad (23)$$

Introducing

$$G_m(\theta, \varphi) = G_m(\theta) \cos^2 m\varphi, \quad (24)$$

the power-gain function $G_m(\theta)$ can be expressed by means of the amplitude and of the total power reflection coefficients

$$G_m(\theta,) = \left[8k \left| \sum_{l=1/0}^{N} A_{ml} d_{ml} \right|^2\right] \cdot \left[a^2 \left\{ \sum_{l=1/0}^{N_m} \mathcal{W}(m,l)\gamma_{ml} \left[|A_{ml}|^2 (1 - r_{ml}^{tot}) - \sum_{\substack{n,k,l \\ k\neq n}}^{N_m} \gamma_{ml} A_{mn} A_{mk}^* R_{mnl} R_{mkl}^* \right] \right\}\right]^{-1}. \quad (25)$$

Denominator of the above expression is proportional to the radiated power, so for the multimode excitation $\mathcal{P}_m^{rad} \neq \sum_l \mathcal{P}_{ml}^{rad}$.

For the single mode excitation, the power-gain function can be expressed by means of the power reflection coefficients r_{ln},

$$G_{ml}(\theta) = \frac{8k|d_l(\theta)|^2}{a^2 \mathcal{W}(m,l)\gamma_{ml}(1 - \sum_{n=1/0}^{N^m} r_{mln})}, \quad (26)$$

or by means of the total power reflection coefficients r_{ml}^{tot},

$$G_{ml}(\theta) = \frac{8k|d_{ml}(\theta)|^2}{a^2 \mathcal{W}(m,l)\gamma_{ml}(1 - r_{ml})}. \quad (27)$$

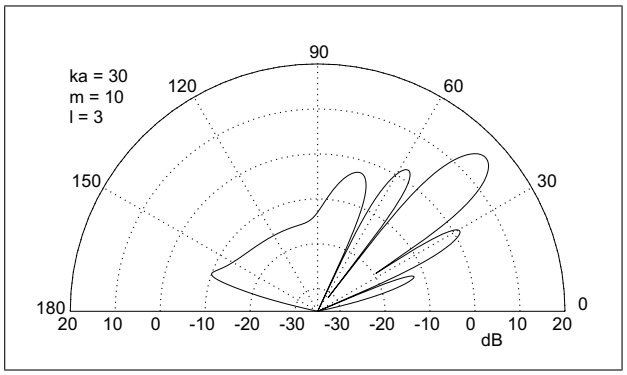

Figure 10. Power-gain function $G_{10,3}(\theta)$ for the diffraction parameter $ka = 30$ slightly below the cut-on frequency of the $(10, 6)$ mode.

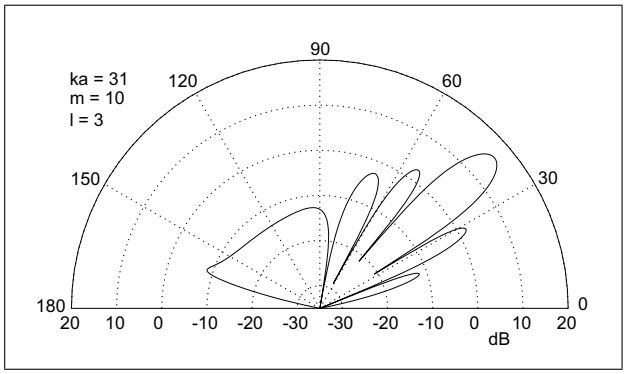

Figure 11. Power-gain function $G_{10,3}(\theta)$ for the diffraction parameter $ka = 31$ slightly above the cut-on frequency of the $(10, 6)$ mode.

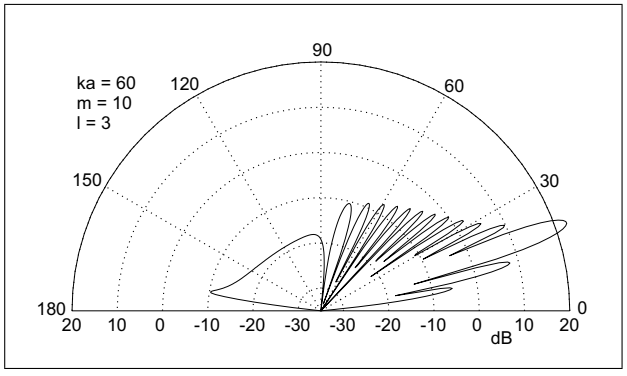

Figure 12. Power-gain function $G_{10,3}(\theta)$ for the diffraction parameter $ka = 60$ above the cut-on frequency of the $(10, 15)$ mode.

Figures 9 - 16 present the power-gain function directivity patterns in the decibel scale (dB). Figure 9 shows the power-gain function of the mode of azimuthal and radial order $m = 40$, $l = 2$, respectively, at $ka = 100$. The number of radiation maxima is equal to the number of the cut-on modes, but the second consecutive maximum, corresponding to the mode radial order exceeds all the others (main lobe). Directivity of modes of high azimuthal order m at large ka gain much interest because of the possible applications in aeroacoustics, especially in modeling of

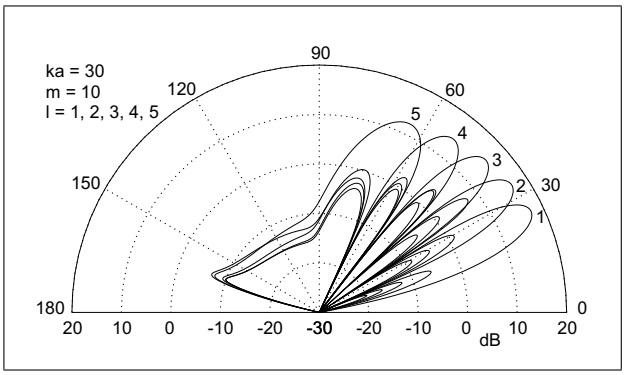

Figure 13. Power-gain function $G_{10,l}(\theta)$ for the diffraction parameter $ka = 30$, $m = 10$ and $l = 1, 2, 3, 4$. Numbers by the curves represent corresponding l values.

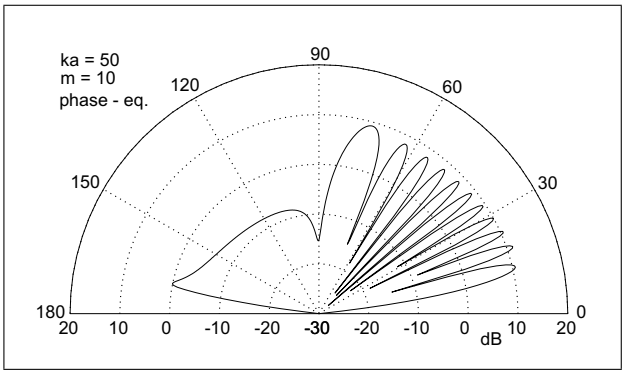

Figure 14. Power-gain function $G_{10}(\theta)$ for the multimode excitation and diffraction parameter $ka = 50$ with amplitudes selected according to the assumption on energy equipartition and equal phases.

sound field generated by turbofan engines. Figures 10–12 present directivity of the power-gain function of the same mode ($m = 10, l = 3$) for different values of ka. Figure 10 is plotted for $ka = 30$, close to but still below the cut-on frequency of the $(10, 6)$ mode, while in Figure 11 $ka = 31$ and so it slightly exceeds the cut-on frequency of the $(10, 6)$ mode. Comparing directivity characteristics in Figure 10 and Figure 11, it may be observed that because of small variation of the ka parameter the direction and amplitude of the main radiation lobe did not change significantly, the feature being in accordance with theoretical findings [23]. For $ka = 60$ the number of modes increases up to fifteen and so does the number of radiation lobes, as can be seen in Figure 12. Figure 13 presents the power-gain directivity characteristics for all propagating modes for $m = 10$ and $ka = 30$ and shows the increase of the main lobe deviation from the axis with incresing of the mode radial order.

On Figures 14–16 the multimode excitation is presented for the diffraction parameter $ka = 50$, amplitudes selected according to the assumption on the energy equipartition (17) and phases: equal (Figure 14), differ between each two consecutive modes by $2\pi/N_m$ (Figure 15) or by π (Figure 16). These directivities differ substantially, indicating their strong dependence on mode phases. For con-

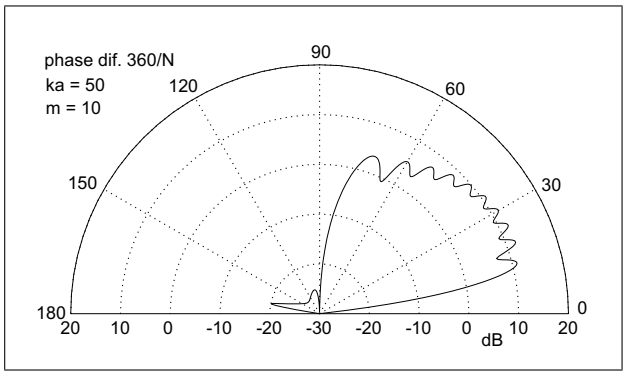

Figure 15. Same as in Figure 14, but with phases of each two consecutive modes differing by $2\pi/N_m$, where N_m is the number of cut-on modes.

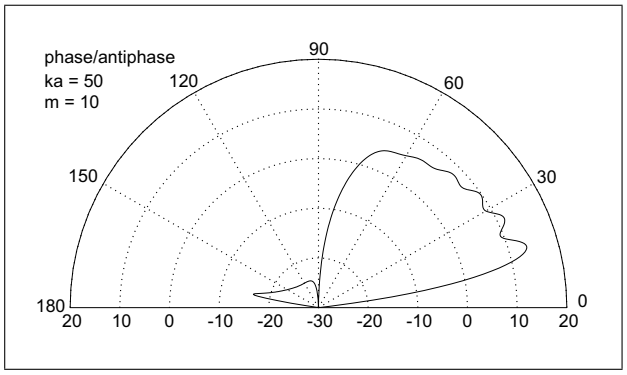

Figure 16. Same as in Figure 14, but with phases of each two consecutive modes differing by π.

secutive modes in anti-phase (Figure 15), for a given azimuthal angle φ nearly uniform radiation in a certain angle θ is observed. Analysis of these and other graphs, not included in this paper, leads to the conclusion that considering noise coming out from a duct at large ka one must not neglect the effect of the higher modes radiation and diffraction on spatial energy distribution, in particular at directions far from the symmetry axis.

The results obtained for the power-gain function $G_m(\theta, \varphi)$ have been verified by calculating its integral over the total solid angle. The results are very encouraging — for the single mode excitation we have obtained values $4\pi(1 \pm 0.001)$, for multimode excitation — $4\pi(1 \pm 0.04)$, while the theory predicts the value of 4π. For the multimode excitation, according to (25), calculations involve summation of complex directivity functions d_{ml}, arguments of which are given by the so-called $Y(\ )$ function (compare cf. Weinstein [4] or Hocter [9]). Computation of this function, involving integration of the argument of the Hankel's function derivative $H_m^{'}(\ )$ in infinite limits can be the source of additional numerical errors. Note that, according to (26) derivation of the argument of the d_{ml} function does not count when computing single mode excitation.

4. Conclusions

The results presented in this paper pertaining to energy distribution in the acoustic field of a circular hard walled duct are based on analytical solution of the wave equation accounting for the incident wave diffraction at the opening. The incident wave is assumed to be multimodal, in order to reflect propagation conditions in large ducts such as jet engine casings, heating, air-conditioning or ventilation systems etc. For the sake of quantitative description of the field the assumption on equal energy distribution between modes heading the duct end was applied. The paper outlines also the procedure for extending the results obtained by applying the Prandtl-Glauert transformation to the duct with uniform velocity profile flow, what in turns allows to model radiation generated by the inlet of a turbofan engine. It follows from the solution of the wave equation that at the duct outlet each mode is not only reflected but also transformed into all modes of the same circumferential order. The power reflection/transformation coefficients and the so-called the total energy reflection coefficients, the last one determining the amount of energy that returns to the waveguide in the form of a selected mode, were derived theoretically and analyzed numerically on graphs. The graphs presenting the power radiated outside versus the diffraction parameter/reduced frequency ka determine intervals in which reflection is negligible and practically the whole power of the incident wave is radiated outside. The results may be useful in modeling of efficient active or passive noise reducing systems, being nowadays a subject of much concern and scientific activity aimed at attenuation of high power carrying modes. The power-gain function which describes to what extent the power distribution in the far field differs from the omnidirectional one, and thus determines the regions of space into which the strongest radiation occurs that may be harmful for the environment, was analyzed as a function of the polar angle for different modes and diffraction parameter ka. The accuracy of applied numerical methods, tested by means of integration of the power-gain function, turned out to be very good. The theoretical model presented above may also be useful for the purpose of validation in numerical modeling (Boundary Element Method, Finite Element Method, Computational Aero-Acoustics methods, Green's Function Discretization technique etc.) of noise radiated from aero-engines. The results have been presented for azimuthal mode orders up to 40 and the reduced frequency ka up to 100, i.e. within the range securing proper accuracy required in solving practical problems.

References

[1] J. M. Tyler, T. G. Sofrin: Axial flow compressor noise study. Automotive Engineers Transactions **70** (1962) 309–322.

[2] W. E. Zorumski: Generalised radiation impedances and reflection coefficients of circular and annular ducts. J. Acoust. Soc. Am. **54** (1973) 1667–1673.

[3] A. Snakowska, R. Wyrzykowski: Calculations of the acoustical field in a semi-infinite cylindrical wave-guide by

means of the Green function expressed in cylindrical coordinates. Archives of Acoustics **11** (1986) 261–285.

[4] L. A. Weinstein: The theory of diffraction and the factorization method (generalised Wiener-Hopf technique). Golem Press, Boulder, Colorado, 1969.

[5] C. J. Chapman: Sound radiation from a cylindrical duct. Part 1. Ray structure of the duct modes and of the external field. J. Fluid. Mech. **281** (1994) 293–311.

[6] C. J. Chapman: Caustics in cylindrical ducts. Proc. R. Soc. Lond. A **455** (1999) 2529–2548.

[7] J. B. Keller: A geometrical theory of diffraction. Proc. Symp. Appl. Math. **8** (1958) 27–52.

[8] J. B. Keller: Geometrical theory of diffraction. J. Opt. Soc. Am. **52** (1962) 116–130.

[9] S. T. Hocter: Sound reflection into a cylindrical duct. Proc. R. Soc. London, Series A **456** (2000) 2707–2716.

[10] S. T. Hocter: Sound radiated from a cylindrical duct with Keller's geometrical theory. J. Sound Vib. **231** (2000) 1243–1256.

[11] S. T. Hocter: Exact and approximate directivity patterns of the sound radiated from a cylindrical duct. J. Sound Vib. **227** (1999) 397–407.

[12] N. Peak: On applications of high-frequency asymptotics in aeroacoustics. Phil. Trans. R. Soc. London, Series A **362** (2004) 673–696.

[13] G. M. Keith, N. Peak: High-wavenumber acoustic radiation from a thin-walled scarfed cylinder. J. Sound Vib. **255** (2002) 147–160.

[14] P. Joseph, P. A. Nelson, M. A. Fisher: Active control of fan tones radiated from turbofan engines. I. External error sensors. J. Acoust. Soc. Am. **106** (1999) 766–778.

[15] A. Snakowska, H. Idczak: Prediction of turbofan engine noise considering diffraction at the duct outlet. Archives of Acoustics **33** (2008) Supplement.

[16] S. Lidoine, H. Batard, S. Troyes, A. Delnevo, R. M.: Acoustic radiation modelling of aeroengine intake comparison between analytical and numerical methods. AIAA-2001-2140 AIAA/CEAS Aeroacoustics Conference and Exhibit, 7th, Maastricht, 2001, Collection of Technical Papers 1.

[17] P. Joseph, C. L. Morfey: Multimode radiation from an unflanged, semi-infinite circular duct. J. Acoust. Soc. Am. **105** (1999) 2590–600.

[18] R. Boucheron, H. Bailliet, J. C. Valiere: Analytical solution of multimode acoustic propagation in circular ducts with laminar mean flow profile. J. Sound Vib. **292** (2006) 504–518.

[19] A. Snakowska: On the principle of equipartition of energy in the sound field inside and outside a circular duct. Acustica **79** (1993) 155–160.

[20] H. Levine, J. Schwinger: On the radiation of sound from an unflanged circular pipe. Phys. Rev. **73** (1948) 383–406.

[21] M. J. Lighthill: Waves in fluids. Cambridge University Press, Cambridge, 2007.

[22] A. Snakowska: The acoustic far field of an arbitrary Bessel mode radiating from the semi-infinite unflanged cylindrical wave-guide. Acustica **77** (1992) 53–62.

[23] G. F. Homicz, J. A. Lordi: A note on the radiative directivity patterns of duct acoustic modes. J. Sound Vib. **41** (1975) 283–290.

[24] G. N. Watson: A treatise on the theory of Bessel functions. Cambridge University Press, Cambridge, 1958.

[25] Lord Rayleigh: The theory of sound. Dover, New York, 1945. (reprinted).

[26] U. Bolleter, M. Crocker: Theory and measurment of modal spectra in a hard-walled cylindrical duct. J. Acoust. Soc. Am. **51** (1972) 1439–1447.

[27] A. Snakowska, H. Idczak, B. Bogusz: Modal anlysis of the acoustic field radiated from an unflanged cylindrical duct – theory and measurement. Acustica united with Acta Acustica **82** (1996) 201–206.

[28] A. Snakowska, H. Idczak: The acoustic power radiated from the outlet of a hard-walled circular duct – theory and measurement. Acta Acustica **3** (1995) 119–128.